Elsevier Editorial System(tm) for Journal of Food Engineering
Manuscript Draft

Manuscript Number: JFOODENG-D-14-00242

Title: Radio-Frequency Thawing of Food Products - A Computational Study

Article Type: Research Article

Keywords: Thawing, radio-frequency, modeling, phase change, meat

Corresponding Author: Dr. Francesco Marra, PhD, MSc

Corresponding Author's Institution: University of Salerno

First Author: Rahmi Uyar

Order of Authors: Rahmi Uyar; Tesfaye F Bedane; T. Koray Palazoglu; Ferruh Erdogdu; Karim W Farag; Francesco Marra, PhD, MSc

Abstract: Main goal of optimal thawing is to minimize thawing time, with least damage to the quality of frozen food product. Microwave (MW) and radio frequency (RF) applications have potential for their use in industrial thawing. Higher penetration depths of RF contribute to a better distribution of energy generated by the interaction between food and electromagnetic field and, thus, help to improve heating uniformity and minimize runaway heating. Modeling is one way to design and optimize such process where complexities due to coupling heat transfer with phase change and solution of electric field are faced. Therefore, the objectives were to develop a computational model to determine temperature distribution in frozen lean beef during thawing and experimentally validate. For this purpose, a commercial software, based on finite element method, was used to solve coupled heat conduction and electric field in 3D domain with temperature dependent thermo-physical and dielectric properties. Experimental data were obtained in 50 Ώ and free-running oscillator RF systems with various sized samples. Comparison of simulation results agreed well with experimental data. The mathematical model might be used for designing RF systems to mitigate the effect of overheating at the surfaces of the sample.

Cover Letter

Fisciano, SA, February the 27th, 2014

Dear Editor,

Please find attached to this message a manuscript titled "Radio-Frequency Thawing of Food Products - A Computational Study", that is the product of a true international cooperation, involving researchers from four different institutions, respectively from UK, Turkey and Italy

In the last years, mathematical model acquired the status of a virtual laboratory and many processes are - nowadays - designed and engineered also thanks to preliminary analysis performed by means solution of mathematical model. In case of radio-frequency thawing of frozen foods, still there is the need of developing model able to predict the temperature distribution and the thawing time. The work done by my co-authors and myself goes in the direction to fill a lack of information about it.

This paper is addressed to the community of scientists and professionals dealing with electro-heating food processes but also developers of simulation tools for the food industry.

I strongly hope you and the reviewers will find this manuscript to be useful for the scope of Journal of Food Engineering.

I look forward to know your decision about the manuscript and sincerely I remain.

Best regards,

Francesco Marra

*Highlights (for review)

Radio-Frequency Thawing of Food Products - A Computational Study

Rahmi Uyar, Tesfaye Faye Bedane, T. Koray Palazoglu, Ferruh Erdogdu, Karim W. Farag and Francesco Marra[2]

Research Highlights

- *Food thawing assisted by RF was modeled and the model was experimentally validated.*
- *Food thawing assisted by RF heating is surely faster than conventional thawing*
- *Hot spots can be a major disadvantage of a RF thawing system.*
- *Optimization methods can help designing better RF system for thawing purposes.*

Radio-Frequency Thawing of Food Products - A Computational Study

Rahmi Uyar[1], Tesfaye Faye Bedane[2], T. Koray Palazoglu[1], Ferruh Erdogdu[3], Karim W. Farag[4] and Francesco Marra[2*]

[1] Department of Food Engineering, University of Mersin, Mersin, Turkey

[2] Dipartimento di Ingegneria Industriale – Università degli studi di Salerno, Salerno, Italy

[3] Department of Food Engineering, Ankara University, Ankara, Turkey

[4]School of Agriculture, Royal Agricultural University, Cirencester, Gloucestershire, United Kingdom

* Corresponding author:

e-mail: fmarra@unisa.it

Tel: +39 089 96 2012

Fax: +39 089 96 4037

Abstract

Main goal of optimal thawing is to minimize thawing time, with least damage to the quality of frozen food product. Microwave (MW) and radio frequency (RF) applications have potential for their use in industrial thawing. Higher penetration depths of RF contribute to a better distribution of energy generated by the interaction between food and electromagnetic field and, thus, help to improve heating uniformity and minimize runaway heating. Modeling is one way to design and optimize such process where complexities due to coupling heat transfer with phase change and solution of electric field are faced. Therefore, the objectives were to develop a computational model to determine temperature distribution in frozen lean beef during thawing and experimentally validate. For this purpose, a commercial software, based on finite element method, was used to solve coupled heat conduction and electric field in 3D domain with temperature dependent thermo-physical and dielectric properties. Experimental data were obtained in 50 Ώ and free-running oscillator RF systems with various sized samples. Comparison of simulation results agreed well with experimental data. The mathematical model might be used for designing RF systems to mitigate the effect of overheating at the surfaces of the sample.

Key-words: Thawing, radio-frequency, modeling, phase change, meat

1. Introduction

Freezing and thawing are important food processing operations. Freezing is one of the key unit operations for preservation of foods. With notable exceptions such as ice cream, frozen foods must be thawed before further use or consumption. In a number of food processing operations, it is a common practice to begin with frozen foods as raw material. For example, in manufacturing sausages, frozen meat is used as the raw material. Similarly, large blocks of frozen fish are processed into fillets for further processing. Different thawing and tempering methods are used for preparing frozen foods for further processing, and each method has its own advantages and disadvantages (e.g., thawing in air or in water, use of impingement systems, microwave thawing). The main goal of a thawing process is to keep thawing time to a minimum so that the least damage is caused to the quality. However, a number of quality attributes might be adversely affected during thawing by moisture (drip) loss, change in the structure of proteins, microbial growth and textural changes.Thawing of large-size frozen foods such as big chunks of meat or fish takes excessively long time in conventional processes like use of still-air or low-velocity moving air environment. This is due to the fact that thawing involves a conduction mode of heat transfer within the product, and upon thawing of outer surfaces, the frozen parts are being surrounded by a low thermal conductivity layer. This slows down the process with inevitable losses in the quality like excessive water loss due to dripping or evaporation and increased microbial growth on the food surface.

Use of conventional methods remain widely used industrial practice primarily because they are economical and applicable to a wide range of products. However, there is a critical need to develop procedures that would reduce thawing time without incurring microbial growth or other adverse physical or chemical changes in the product. As noted by Farag et al. (2008a), industry is always interested in fast and compact systems while maintaining the quality during thawing. Besides conventional thawing systems of using air, microwave (MW) and radio frequency (RF) applications appear to have the potential for industrial use (Farag et al., 2008a) to overcome the various problems. In these systems, heat generation is carried out by dipole rotation and ionic polarization through the movement and friction of diploes and/or ions under alternating electric field (Buffler, 1993).In dielectric heating, dipole rotation is major contributor at higher frequencies (MW - 915 or 2450 MHz) whilst ionic displacement is more pronounced at the lower frequencies of RF (e.g., 27.12 MHz) (Jones, 1992). MW heating is more accepted for rapidly heating small sized products but found to be less satisfactory for heating larger sized food products (Taher and Farid, 2001). This is due to the problem of runaway heating (occurs with melting of ice since water heats faster due to its high dielectric loss factor) leading to a non-uniform heating (some parts might be cooked with some parts still unfrozen) and limited penetration depth compared to RF heating (Buffler, 1993).Higher penetration depths of RF and less generated energy to convert heating help improve heating uniformity and minimize the runaway heating problem. Besides experimental studies, mathematical modeling is another way to design and optimize an RF process.

Modeling RF processes is a multi-physics problem, and it is generally built for solving electromagnetic equation coupled with heat transfer equation with a generation term as a function of electric field. Various studies in the literature focused on modeling of RF processes to improve heating uniformity(Chan et al., 2004; Yang et al., 2004;Marra et al., 2007; Romano and Marra, 2008; Birla et al., 2008; Petrescu and Ferariu, 2008; Wang et al., 2012).The coupled electro-thermal problem of modeling an RF process becomes more complicated for simulation of thawing since the phase change process requires dealing with evolving large latent heat over a small range of temperature. Moreover, the changes in thermo-physical and dielectric properties in phase change region also increase the complexity of RF thawing simulation. To deal with this difficulty, apparent specific heat, enthalpy and quasi-enthalpy methods are suggested (Pham, 2006). Then, simulation of an RF thawing process becomes a multi-physics problem where the coupled heat transfer with electrical field distribution should be solved including the phase change process. There are not many studies for modeling RF thawing carried out in the literature for this purpose while modeling MW thawing has been practiced (Basak and Ayappa, 1997; Chamcong and Datta, 1999a, b; Taher and Farid, 2001; Rattanadecho, 2004; Tilford et al., 2007; Campanone and Zaritzky, 2010). Therefore, the objectives of this study were to:

- Develop a computational model to determine the electrical field distribution in a RF system and temperature distribution in the frozen product during thawing;
- Validate the thawing model with experimental results.

2.Materials and Methods

The study was completed in two parts. First, a computational 3D multi-physics model for modeling RF thawing was developed using COMSOL (Comsol V4.3b, Comsol AB, Stockholm, Sweden) for parallel-electrode RF systems, and the model was validated with two various sets of experimental data. The first set of experimental data was obtained from literature (Farag et al., 2011) in which a custom built RF system (50 Ω) was used to thaw a large size sample of frozen lean beef meat (≈3.84 kg).A series of experiments was carried out for the second data set in a free-running oscillator RF system for thawing smaller samples of frozen ground lean beef.

The $50\,\Omega$ technology and free-running oscillators are two different designs used in food industry. These systems were reported to gain popularity due to their offering superior frequency stability and better compliance with electro-magnetic compatibility (EMC) regulations (Orsat and Raghavan, 2005). Jiao et al. (2014) explains that the free-running oscillator systems are the most commonly used systems due to low cost, simple structure and flexibility while $50\,\Omega$ systems use modern methods to control frequency and power. In free-running oscillator systems, amount of the power converted to heat energy depends on the material properties (Rowley, 2001). Hence, the experimental data obtained in both systems were used in the model validation studies.

2.1. Experimental Methodology

The details of experimental data for thawing of large size lean beef (20×20×10 cm) were given in Farag et al. (2008 and 2011) where temperatures measurement at 25 different locations (Fig.1b) were recorded and the average value of these were used to represent the temperature profile during thawing.In this study, two RF systems were considered. The first one, related to the studies published by Farag et al. (2008a and b, 2010, 2011), is a custom built $50\,\Omega$- 400 W system (Chester, UK) using a low power generator with an automatic impedance matching network and controller at a frequency of 27.12 MHz was used. The boxed frozen lean beef sample (20×20×10 cm) was placed at the center of the bottom electrode (Fig. 1a) during the experiments. The distance between sample and upper electrode was 1.4 cm.

The second RF system, that has been used in this study, is a 2kW pilot scale free-running oscillator RF system (Fig. 2a - Sonar, Izmir, Turkey). Itwas used to generate the experimental data. For this purpose, minced lean beef was purchased from a local store. Samples in two various dimensions were prepared for RF thawing studies: 12.0×17.2×3.8 cm - 0.8 kg; 12.0×17.2×5.5 cm - 1.2 kg (Fig. 2b). These samples were placed then in a poly-propylene (PP) cup (PP), two fiber-optic probes were placedin the samples (Fig. 3), and they were frozen in a freezer (some samples at -13°C, some other at -18°C) prior to the thawing experiments. For the first block, the distance between sample surface and upper electrode was 12 cm while it was 13 cm for the latter one. Smaller size samples were specifically chosen to validate the simulation results since the data for a larger case was already obtained from the literature as explained above.Experiments on smaller size samples were performed to investigate about the effects of sample size on RF power absorption, since sample size may have a major effect on RF power absorption, as demonstrated by a recent study (Uyar et al., 2014).

To demonstrate the effect of RF thawing compared to conventional natural convection thawing, upon the completion of RF thawing study, one of the blocks were re-frozen and then left to thaw under room temperature. There was a possibility of changing the thermal-physical properties in the freeze-thaw cycle. However, thawing time difference between RF thawing and conventional thawing was so large that the possible change in the properties would not cause this kind of time difference, and again the idea was just to demonstrate the effect of RF thawing.

2.2. Computational Method

RF thawing simulations were performed considering the apparatus configuration used by some of the authors in the past (Farag et al., 2010), it being a parallel plate RF systems consisting of a chamber with electrically insulated walls and of two parallel rectangular electrodes (Figs. 1a and 2a). To determine the electric field distribution inside the RF system and temperature change in the product, solution of Fourier heat transfer equation plus a generation term, coupled with the quasi-static electro-magnetic field equations, in addition to handling the phase change, was required:

$$\rho\, c_p \frac{\partial T}{\partial t} = \nabla \cdot k \nabla T + Q_{abs} \qquad (1)$$

where ρ is density, c_p is specific heat, k is thermal conductivity, t is time, T is the temperature, and Q_{abs} is the RF power absorbed per unit of volume by the load. Being Q_{abs} generated by the electric field distribution, its expression is:

$$Q_{abs} = 2\pi f \varepsilon_0 \varepsilon'' \left|\overline{E}\right|^2 \qquad (2)$$

where f is the frequency of the radio-wave generator, ε_0 is the permittivity of free space, ε'' is the relative dielectric loss factor of the sample load, and $\left|\overline{E}\right|$ is the modulus of the electric field. Electric field within the sample load and voltage potential at any point inside the electrodes are given by Gauss law derived from a quasi-static approximation of Maxwell's equations:

$$\nabla\left(\varepsilon \cdot \overline{E}\right) = 0 \qquad (3)$$

where ε is permittivity of the load (relative permittivity related to dielectric constant, ε' and dielectric loss factors, ε'') and $\overline{E}$ is the electric field vector. Modeling of RF heating as a quasi-static electric field between the electrodes will be preferred since the electrode sizes would be very small compared to the wavelength at 27.12 MHz (≈11 m in free space) (Marra et al., 2007). Since solution to Eq. 1 is also required within the load, Gauss law is applied for the air space between electrodes including the sample load and air around it.

2.2.1. Thermophysical and dielectric properties

Due to the fact that phase change in some food substances occurs over a range of temperature (Pham, 2006) and large latent heat evolves over this range, special techniques were required to deal with such problems. Pham (2006) reviewed and presented the possible techniques to deal with such problems as apparent specific heat, enthalpy and quasi-enthalpy methods. Based on this, apparent specific heat method was applied in this study considering the specific heat values (expressed as J kg^{-1} K^{-1}) in three regions (frozen, phase change and unfrozen) as described below:

$$\begin{array}{ll} T \le T_{m1} & c_p = c_{p,\,frozen} = 1935.2 \\ T_{m1} \le T \le T_{m2} & c_p = \dfrac{c_{p,\,frozen} + c_{p,\,frozen}}{2} + \dfrac{\lambda}{T_{m2} - T_{m1}} = 153016.3 \\ T > T_{m2} & c_p = c_{p,unfrozen} = 3497.4 \end{array} \quad (4)$$

where T_{m1} and T_{m2} are the initial and final temperature during phase change process, $c_{p,frozen}$ and $c_{p,unfrozen}$ are the specific heat values for frozen and unfrozen cases, and λ is the latent heat.These values were derived using the data reported by Farag et al. (2008b). Samara et al. (2012) also used the same approach, as suggested by Groulx and Ogoh (2009),to model the natural convection driven melting of a phase change material. A similar step function was also used for temperature dependency of density where the density values were 961 $(T \le T_{m1})$, 1007

$\left(T_{m1} \le T \le T_{m2}\right)$ and 1053 $\left(T > T_{m2}\right)$ kg/m³.Detailed explanation for density calculation using the proximate composition of lean beef was given in Bedane (2013).

All the other required data for thermophysical and dielectric properties (thermal conductivity-k, relative dielectric constant-ε' and relative dielectric loss factor-ε'') were obtained from Farag et al. (2008b) as a function of temperatureare shown in Fig. 4 (dielectric properties) and Fig. 5 (thermal conductivity). It has been well known that, for a given material, the dielectric properties might vary during heating via the temperature increase, and this behavior changes the heating rate accordingly. Even though the dielectric properties of various food materials as a function of temperature have been reported in the literature (Lyng et al., 2005; Sosa-Morales et al., 2010), the available data in the frozen range was scarce. Hence, the available data reported by Farag et al. (2008a; 2011) were applied in the simulations. As noted by Jiao et al. (2014), the best case scenario would be to know the dielectric properties as a function of temperature, moisture content and other properties before conducting simulations and model validation experiments.

2.2.2. Boundary conditions

Boundary conditions for Gauss law to determine the electric field distribution inside the system were:

- upper electrode was maintained at a certain potential $\left(V_0\right)$ according with the applied output power with a frequency of 27.12 MHz (even though the voltage varies all over the surface of the top electrode, it was assumed to be uniform since the electrode dimensions were much lower than 30% of the RF wave length, ≈11 m; Tiwari et al., (2011) and constant during the processing time),

- lower electrode was maintained at the ground condition $(V = 0)$, and
- side walls were electrically insulated $(\nabla\overline{E} = 0)$.

Boundary conditions for Fourier heat transfer equation to determine temperature distribution inside the sample load were:

- Convective heat transfer was considered on the external surfaces:

$$-n \cdot k\nabla T = h(T - T_{air}) \tag{5}$$

  where *h* is the convective heat transfer coefficient $\left(h = 10\dfrac{W}{m^2K}\right)$, and T_{air} is the temperature inside the cavity (≈20 °C), and

- Sample was assumed at uniform initial temperature $T_{0.}$ $(T_0 \approx -13°C, -18°C)$.

3. Results and Discussion

3.1 Simulations

Simultaneous solution of Gauss law and Fourier heat transfer equation with power generation required numerical computation. For this purpose, a finite element based software - COMSOL (Comsol V. 4.3b, Comsol AB, Stockholm, Sweden) was used. Important stages of the numerical solution were defining the domain and sub-domains of interest, defining transport equations, setting up the boundary conditions, describing thermophysical and dielectric properties, preparing the computational geometry (meshing), deciding the numerical solver and solving the problem. After defining the geometry and describing required properties, an unstructured mesh consisting of Lagrange quadratic elements was created over the entire domain of RF cavity. In the mesh convergence studies to very that the results were independent on mesh size, three various mesh sizes (finer, extra fine and extremely fine) were tested. Due to the certain oscillations observed in the temperature change in the phase change region, the extremely fine mesh structure was preferred even though it leads to longer computational times. Regarding the phase change region, the narrower the phase transition interval used to approximate specific heat the larger the jump in the specific heat values and the larger the numerical difficulties encountered during simulations. Optimum phase transition interval of 1.5 and 4 K amplitude were used to simulate for the literature data and the obtained from the free-running oscillator RF system. These values were obtained by observing the experimental data and pre-runs of the simulation models. The difference might be due to the fact the average temperature values were used in the literature data while the temperature data obtained at certain locations were used in the latter case.

The simulations were performed on a workstation Intel(R) Core(TM) i7 CPU Q720 @ 1.60 GHz; equipped with a RAM of 24 Gb DDR3. The workstation runs under Windows 7 Professional operating system. Simultaneous solution of the coupled transient equations took 10598 s (≈3 h) for 3000s of RF thawing process with free time stepping for the literature case (Farag et al. 2011) while it took 240384 s (≈2.8 days) for the case of 2400 s thawing time of 12.0×17.2×5.5 cm sample. The number of the elements was 285629 for the literature case while it was 7109745 for the latter case (geometries given Fig. 1b and Fig. 2a). Since the pre-runs with smaller fixed time steps did not improve the results and reduce the possible oscillations in the temperature. free time-stepping was used in all the simulations. For solving the differential equation sets, the direct linear system solver UMFPACK was used with a relative tolerance and an absolute tolerance of 0.01 and 0.001, respectively.

3.2. Experimental validation of simulation results

Fig. 6 shows the comparison of simulation results with the experimental data obtained by Farag et al. (2011) where average temperature from 25 locations (as demonstrated in Fig. 1b) in the sample. Because of the limitation of available experimental data, only temperature data in the tempering region were used in this part of the validation studies. Tempering was reported to be more commonly used for products that would require a further size reduction to reduce problems associated with thawing such as drip loss and microbial growth due to the rather shorter time (Farag et al., 2008a). Meat products, in addition, becomes highly available to mechanical chopping after tempering (James and James, 2002). Temperature contours in the zx plane at the thawing time of 600 and 3000 s are demonstrated in Fig. 7. As observed, a rather uniform temperature is obtained towards the end of the thawing time demonstrating the significant effect of RF on obtaining uniform temperature inside the product.In this simulation, the voltage level along the upper electrode was 141.42 V.

The comparison between simulation results and the experimental data obtained in the system (Fig.2) for a frozen ground lean beef block of 12.0×17.2×3.8 cm and 12.0×17.2×5.5 cm is shown in Fig.8 and Fig.9 respectively. The experimental data were obtained at two points in these systems (Fig. 2b), and the distance between the upper electrode and the sample surface was 12 and 13 cm, respectively. In this free-running oscillator RF system, the voltage along the upper electrode was determined to be 1375 V. As suggested by Marshall and Metaxas (1998), Birla et al. (2008),Tiwari et al. (2011) and Alfaifi et al. (2014), various input voltage values were tried to predict a realistic transient temperature that would fit with the experimental data. As a result of numerous simulations within a certain range of voltage level, 1375 V along the upper electrode was selected. It was not practical to measure the voltage without distorting the electric field during the operation of an RF system (Marshall and Metaxas, 1998). As reported by Metaxas (1996), the voltage varies 7% between standby and full load in a typical industrial scale system. Hence, a constant electric potential on the upper electrode was assumed to be a realistic assumption.

As observed in Figs. 6, 8 and 9, the simulation results agreed well with the experimental data. However, there were certain discrepancies in Figs. 8 and 9 where the local temperature data were obtained in the 2 kW free-running oscillator system (Sonar, Izmir, Turkey). For these comparisons, voltage level on the upper electrode was determined through a trial-error procedure as explained above. However, the experimental data in Fig. 6 was the average temperature obtained as shown in Fig. 1b. The experimental uncertainty might also be a point to consider for the discrepancies observed in Figs. 8 and 9. Tilford et al. (2007) listed explanations on the discrepancy of simulation results compared to the experimental data. These were based on the non-linear dielectric properties around the phase change region and numerical errors. The electric potential distribution inside the system is shown in Fig. 10 for the case of 12.0×17.2×5.5 cm sample. The highest electric potential was along the upper electrode while the top regions of the system also experienced a certain electric potential distribution. This distribution was also experimentally observed to be high enough to light a halogen lamp. This shows a certain amount of electric potential cannot be used to be beneficial in thawing, and this information might further be used for design and optimization purposes.

3.3. Effect of sample size and power absorption of samples on thawing time

As demonstrated by Uyar et al. (2014), the sample size has significant effect on the power absorption during the RF heating. In this study also, RF power absorption was observed to be higher for large sized block and as a result the thawing time was observed to be shorter. Time wise integrated absorbed power amount was 35.58 W for the block of 12.0×17.2×3.8 cm while it was around 4 times of this value for the larger block of 12.0×17.2×5.5 cm (140.73 W). Based on this difference, thawing time was more than 3 times shorter for the larger block. In conventional thawing systems, due to the significant effect of conduction heat transfer inside the product and convection heat transfer outside (as noted in the introduction section, upon thawing of outer surfaces at the initial stages of a conventional thawing process, still-frozen inside parts are being surrounded by a low thermal conductivity layer leading to longer thawing times), the thawing times are always higher for the larger sizes, and this contradiction makes the RF processes an available industrial process.

With a further effort, another set of experiment was carried out to observe the effect of RF thawing versus a conventional thawing process. Fig. 11 shows the comparison of thawing temperature profile during RF application compared to the conventional natural convection process for the frozen block of 12.0×17.2×3.8 cm lean beef. The distance between the upper electrode and the sample surface was 12 cm during RF application. Farag et al. (2008a) reduced tempering time 30 fold for 4 kg meat blends with a greater uniformity of temperature distribution. Based on the study conducted by Uyar et al. (2014), the sample sizes had a significant effect on power absorption during RF processes, and this might be even more effective for the frozen products due to the dielectric properties of ice. Hence, a smaller size sample was used to compare RF thawing time with conventional natural convective thawing, and ≈3 fold reduction in thawing time can be observed in Fig. 11.

4. Conclusions

Besides conventional thawing systems, electromagnetic applications (MW and RF) appear to have the potential for industrial use to keep thawing time to a minimum with least damage to the quality. MWs, with their limited penetration depth compared to RF, are less satisfactory for thawing of especially the larger sized products due to runaway heating and non-uniform temperature distribution. RF systems might offer better process control for these disadvantages if an optimized process might be developed. The first condition to design and optimize an RF thawing system is the availability of a mathematical model.

In this study, a computational model was developed to determine the electrical field distribution in a50 Ωand a free running oscillator RF system.Temperature and distribution in the frozen lean beef and electric potential distribution inside the system were determined, and the modelswere validated with experimental data for various sized samples. Effect of sample size and power absorption of samples on thawing time were demonstrated while RF thawing was also compared with a conventional way of thawing under still air. Non-uniform temperature distribution during thawing, especially high temperatures encountered along the surface and corners of the product, is a major disadvantage of a RF thawing system.Mathematical models might be used for designing RF systems to mitigate the effect of overheating at the corners via combining them with optimization methods.

5. Acknowledgements

Upon completion of this study, Dr. Erdogdu was affiliated with the Department of Food Engineering at the University of Mersin. He is now affiliated with the Ankara University. He appreciates all the collaborations in Mersin and the valuable time he spent.

Dr. Marra and Dr. Farag express their gratitude to Dr. James G. Lyng for the guidance that he provided to them in the last years working in the area of RF heating of foods.

6. References

Alfaifi, B., Tang, J., Jiao, Y., Wang, S., Raso, B., Jiao, S. and Sablani, S. 2014. Radio frequency disinfestation treatments for dried fruit; model development and validation. Journal of Food Engineering. 120: 268-276.

Basak, T. and Ayappa, K.G. 1997. Analysis of microwave thawing of slabs with effective heat capacity method. AIChe Journal. 43: 1662-1674.

Bedane, T.F. 2013. Mathematical modeling of radio-frequency thawing of foods. M.Sc. Thesis. Università degli Studi di Salerno, Fisciano, SA, Italy.

Birla, S.L., Wang, S., Tang, J. 2008. Computer simulation of radio frequency heating of model fruit immersed in water. Journal of Food Engineering. 84: 270–280.

Buffler, C.H. 1993. Dielectric properties of foods and microwave materials. In *Microwave Cooking and Processing* (pp. 46-49). New York, NY, USA: Van Nostrant Reinhold.

Campanone, L.A. and Zaritzky, N.E. 2010. Mathematical modeling and simulation of microwave thawing of large solid foods under different operating conditions. Food and Bioprocess Technology. 3: 813-825.

Chamcong, M. and Datta, A.K. 1999a. Thawing of foods in a microwave oven: I. Effect of power levels and power cycling. Journal of Microwave Power and Electromagnetic Energy. 34(1): 9-21.

Chamcong, M. and Datta, A.K. 1999b. Thawing of foods in a microwave oven: I. Effect of load geometry and dielectric properties. Journal of Microwave Power and Electromagnetic Energy. 34(1): 22-32.

Chan, T.V.C.T., Tang, J. and Younce, F. 2004. 3-dimensional numerical modeling of an industrial radio frequency heating system using finite elements. Journal of Microwave Power and Electromagnetic Energy. 39: 87-105.

Farag, K.W., Lyng, J.G., Morgan, D.J. and Cronin, D.A. 2008a. A comparison of conventional and radio frequency tempering of beef meats: effects on product temperature distribution. Meat Science. 80: 488-495.

Farag, K.W., Lyng, J.G., Morgan, D.J. and Cronin, D.A. 2008b. Dielectric and thermophysical properties of different beef meat blends over a temperature range of -18 to +10 °C. Meat Science. 79: 740-747.

Farag, K.W., Lyng, J.G., Morgan, D.J. and Cronin, D.A. 2011. A comparison of conventional and radio frequency thawing of beef meats: effects on product temperature distribution. Food and Bioprocess Technology. 4: 1128-1136.

Groulx, D. and Ogoh, W. 2009. Solid-liquid phase change simulation applied to a cylindrical latent heat energy system. *Comsol Conference, 2009*, Boston, USA, 7 p.

James, S.J. and James, C. 2002. Thawing and tempering. In: *Meat Refrigeration* (pp. 159-190). Cambridge: Woodhead Publishing.

Jiao, Y., Tang, J., Wang, S. and Koral, T. 2014. Influence of dielectric properties on the heating rate in free-running oscillator radio frequency systems. Journal of Food Engineering. 120: 197-203.

Jones, P.L. 1992. Dielectric heating for food processing. Nutrition & Food Science. 2: 14-15.

Lyng, J.G., Zhang, L. and Brunton, N.P. 2005. A survey of the dielectric properties of meats and ingredients used in meat product manufacture. Meat Science. 69: 589-602.

Marra, F., Lyng, J., Romano, V. and McKenna, B. 2007. Radio-frequency heating of foodstuff: solution and validation of a mathematical model. Journal of Food Engineering. 79: 998–1006.

Marshall, M.G. and Metaxas, A.C. 1998. Modeling of the radio frequency electric field strength developed during the RF assisted heat pump drying of particulates. Journal of Microwave Power and Electromagnetic Energy. 33: 167-177.

Metaxas, A.C. 1996. *Foundations of Electroheat - A Unified Approach*. 1st Ed. New York, NY, John Wiley & Sons.

Orsat, V. and Raghavan, G.S.V. 2005. Radio-frequency processing. In: *Emerging Technologies for Food Processing*. Sub, D-W. (Ed.). Elsevier Ltd.New York, USA. pp. 445-468.

Petrescu, C. and Ferariu, L. 2008. Modeling of dielectric heating in radio-frequency applicator optimized for uniform temperature by means of genetic algorithms. World Academy of Science, Engineering and Technology.47: 129-134.

Pham, Q.T. 2006. Modeling heat and mass transfer in frozen foods: a review. International Journal of Refrigeration. 29: 876-888.

Rattanadecho, P. 2004. Theoretical and experimental investigation of microwave thawing of frozen layer using a microwave oven (effects of layered configurations and layer thickness). International Journal of Heat and Mass Transfer. 47: 937-945.

Romano, V. and Marra, F. 2008. A numerical analysis of radio frequency heating of regular shaped foodstuff. Journal of Food Engineering. 84: 449–457.

Rowley, A.T. 2001. Radio frequency heating. In: *Thermal Technologies in Food Processing*. Richardson, P. (Ed.). Woodhead Publishing Cambridge. Cambridge, UK. pp. 127-162.

Samara, F., Groulx, D. and Biwole, P.H. 2012. Natural convection driven melting of phase change material: comparison of two methods. *Comsol Conference, 2012*, Boston, USA, 8 p.

Sosa-Morales, M.E., Valerio-Junco, L., Lopez-Malo, A. and Garcia, H.S. 2010. Dielectric properties of foods: reported data in the 21st century and their potential applications. LWT - Food Science and Technology. 43: 1169-1179.

Taher, B.J. and Farid, M.M. 2001. Cyclic microwave thawing of frozen meat: experimental and theoretical investigation. Chemical Engineering and Processing. 40: 379-389.

Tilford, T., Baginski, E., Kelder, J., Parrott, K. and Pericleous, K. 2007. Microwave modeling and validation in food thawing applications. Journal of Microwave Power and Electromagnetic Energy. 41(4): 30-45.

Tiwari, G., Wang, S., Tang, J. and Birla, S.L. 2011. Computer simulation model development and validation for radio frequency (RF) heating of dry food materials. Journal of Food Engineering. 105: 48–55.

Uyar, R., Erdogdu, F, and Marra, F. 2014. Effect of volume on power absorption and temperature evolution during radio-frequency heating of meat cubes: a computational study. Food and Bioproducts Processing. http://dx.doi.org/10.1016/j.fbp.2013.12.005.

Wang, J., Luechapattanaporn, K., Wang, Y. and Tang, J. 2012. Radio-frequency heating of heterogeneous food - meat lasagna. Journal of Food Engineering. 108: 183-193

Yang J, Zhao, Y, Wells, JH. 2003. Computer simulation of capacitive radio frequency (RF) dielectric heating on vegetable sprout seeds. Journal of Food Process Engineering. 26: 239-263.

Figure Legends

Figure 1. (a) Experimental set up used by (adapted from) Farag et al. (2008); (b) 25 locations in the sample where the temperature data were recorded (adapted From Farag et al., 2008).

Figure 2. (a) 2 kW, 27.12 MHz pilot-scale free-runningoscillator RFsystem; (b) meat sample used in the experiments.

Figure 3. Location of the fiber optic probes in the samples (a) frozen sample block of: 12.0×17.2×3.8 cm (b) frozen sampleblock of 12.0×17.2×5.5 cm.

Figure 4. Dielectric properties as a function of temperature (a) Dielectric constant; (b) Dielectric loss factor - (Adapted from Farag et al.,(2008b).

Figure 5. Thermal conductivity (W/m-K) as a function of temperature -(Adapted from Farag et al.,(2008b).

Figure 6. Comparison of simulation results with the experimental data obtained by Farag et al. (2011).

Figure 7. Temperature contours in the zx plane of the lean beef sample at the radio frequency thawing time of (a) 600 s and (b) 3000 s.

Figure 8. Comparison of simulation results with the experimental data for a frozen ground lean beef block of 12.0×17.2×3.8 cm where the distance between the upper electrode and the sample surface was 12 cm.

Figure9. Comparison of simulation results with the experimental data for a frozen ground lean beef block of 12.0×17.2×5.5 cm where the distance between the upper electrode and the sample surface was 13 cm.

Figure 10. Electric potentaial distribution for the case of 12.0×17.2×5.5 cm sample.

Figure 11. Comparison of radio frequency thawing with conventional natural convection thawing (experiments were conducted with the frozen block of 12.0×17.2×3.8 cm lean beef).

Figure01

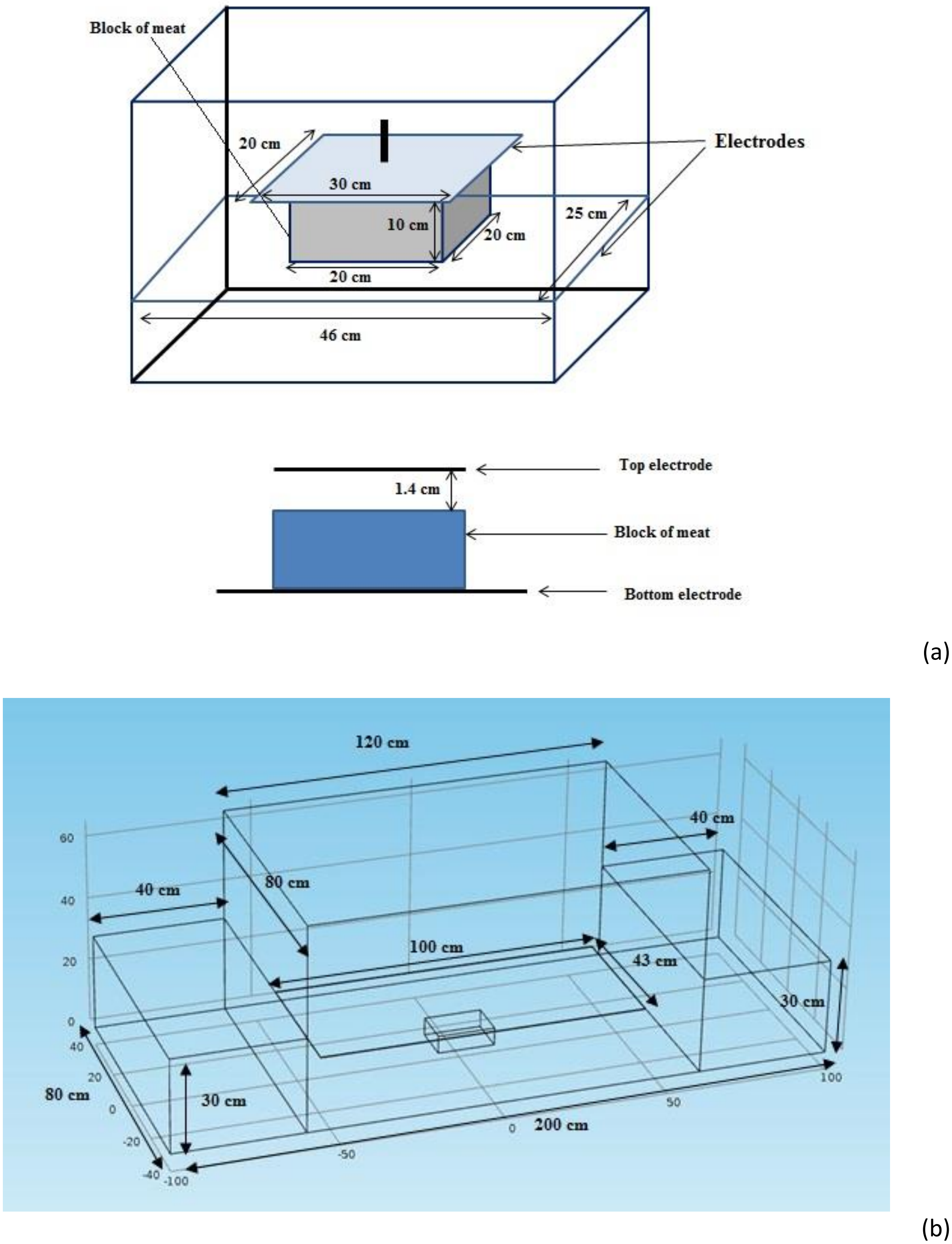

Figure 1. (a) Experimental set up used by (adapted from) Farag et al. (2008); (b) 25 locations in the sample where the temperature data were recorded (adapted From Farag et al., 2008).

Figure02

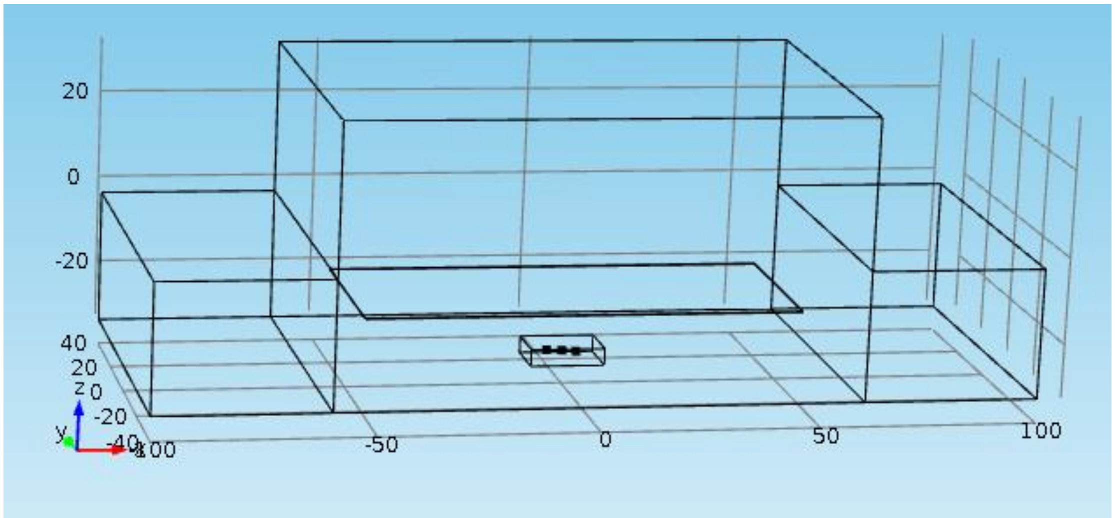

(a)

(b)

Figure 2. (a) 2 kW, 27.12 MHz pilot-scale free-running oscillator RF system; (b) meat sample used in the experiments.

Figure03

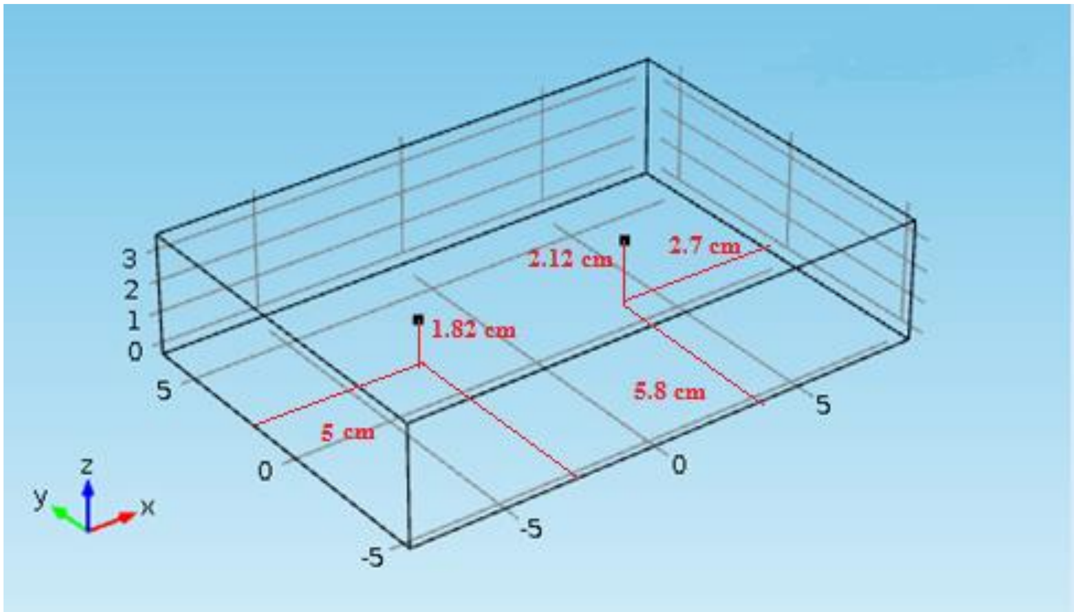

(a)

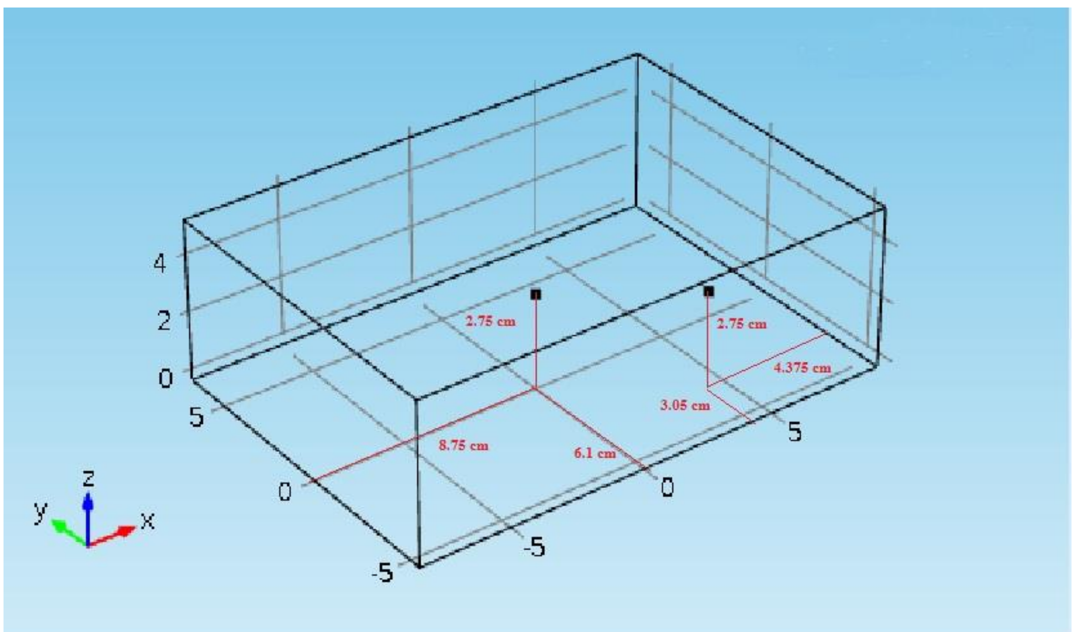

(b)

Figure 3. Location of the fiber optic probes in the samples (a) frozen sample block of: 12.0×17.2×3.8 cm (b) frozen sample block of 12.0×17.2×5.5 cm.

Figure04

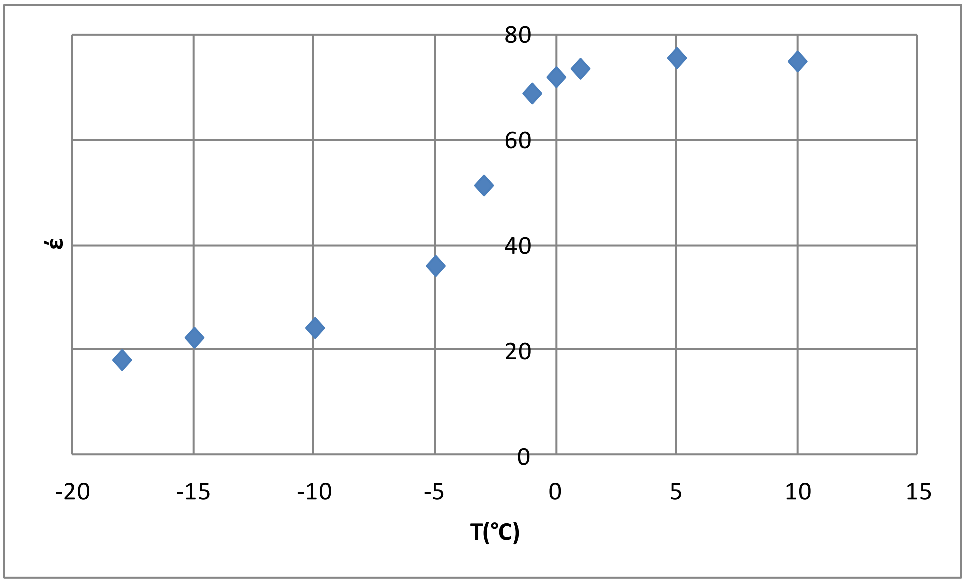

(a)

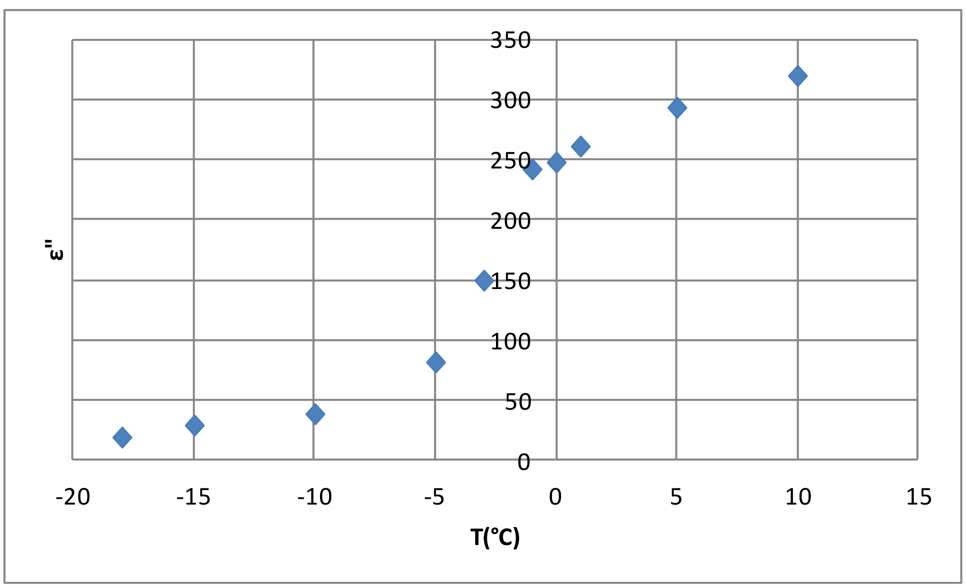

(b)

Figure 4. Dielectric properties as a function of temperature (a) Dielectric constant; (b) Dielectric loss factor - (Adapted from Farag et al.,(2008b).

Figure05

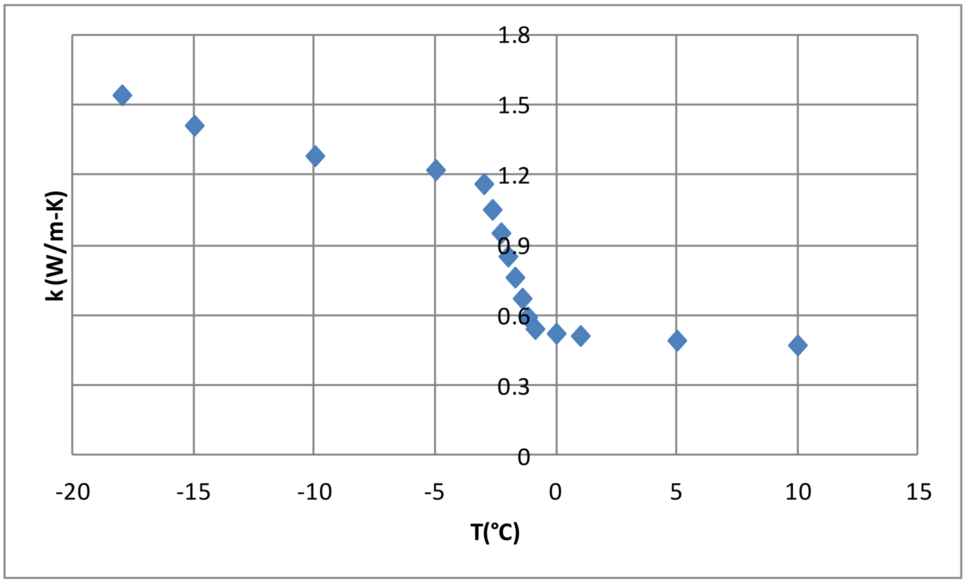

(a)

Figure 5. Thermal conductivity (W m^{-1} K^{-1}) as a function of temperature - (Adapted from Farag et al.,(2008b).

Figure06

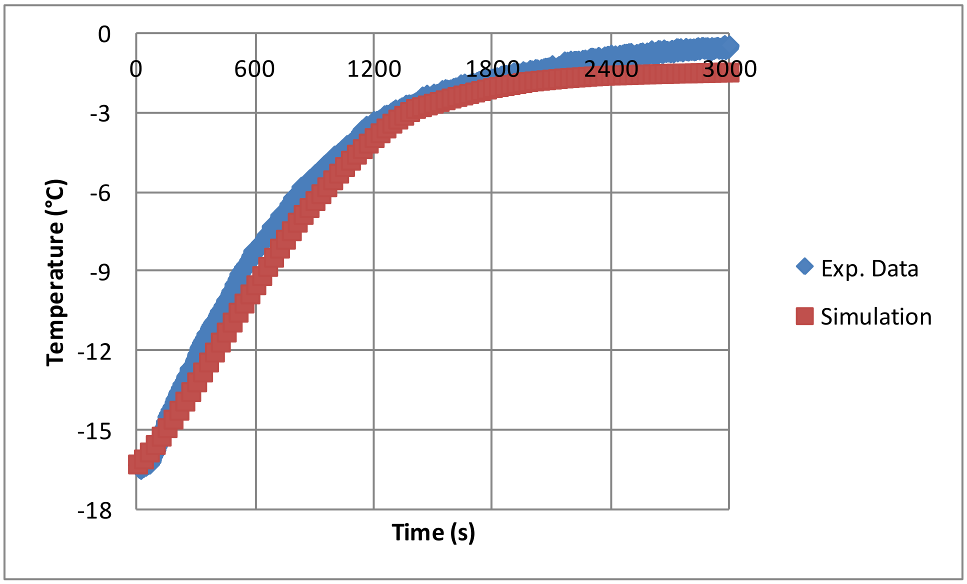

Figure 6. Comparison of simulation results with the experimental data obtained by Farag et al. (2011).

Figure07

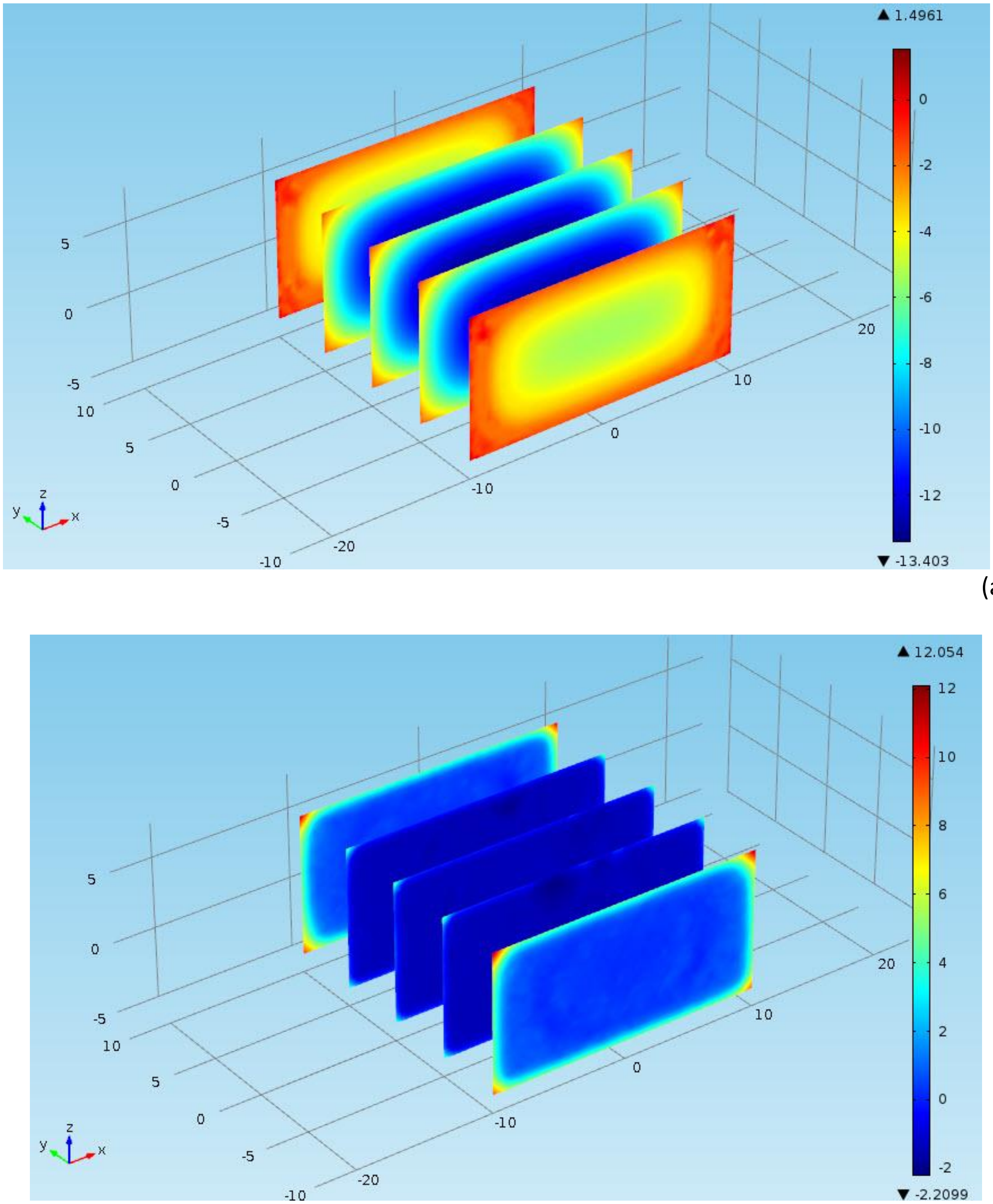

(a)

(b)

Figure 7. Temperature contours in the zx plane of the lean beef sample at the radio frequency thawing time of (a) 600 s and (b) 3000 s.

Figure08

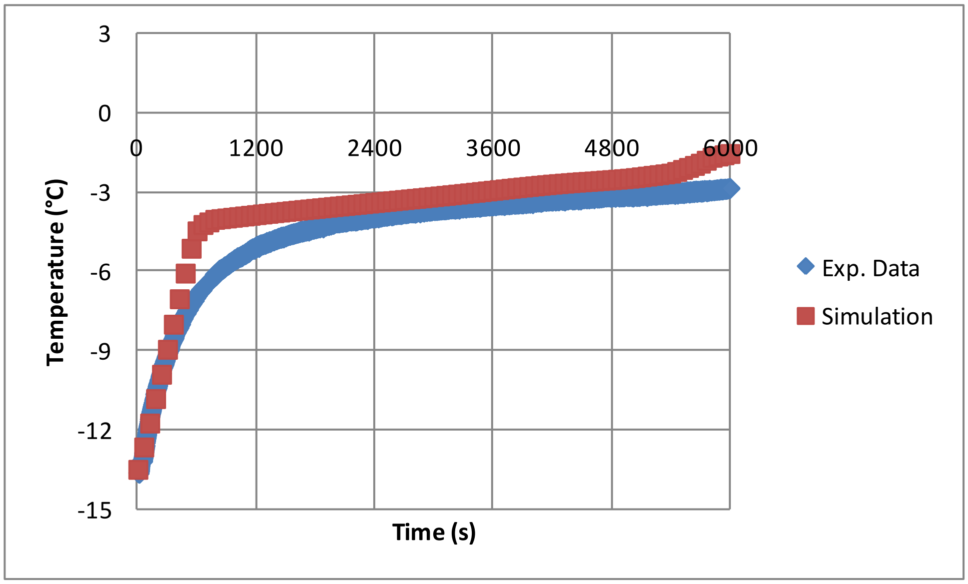

(a) - 496

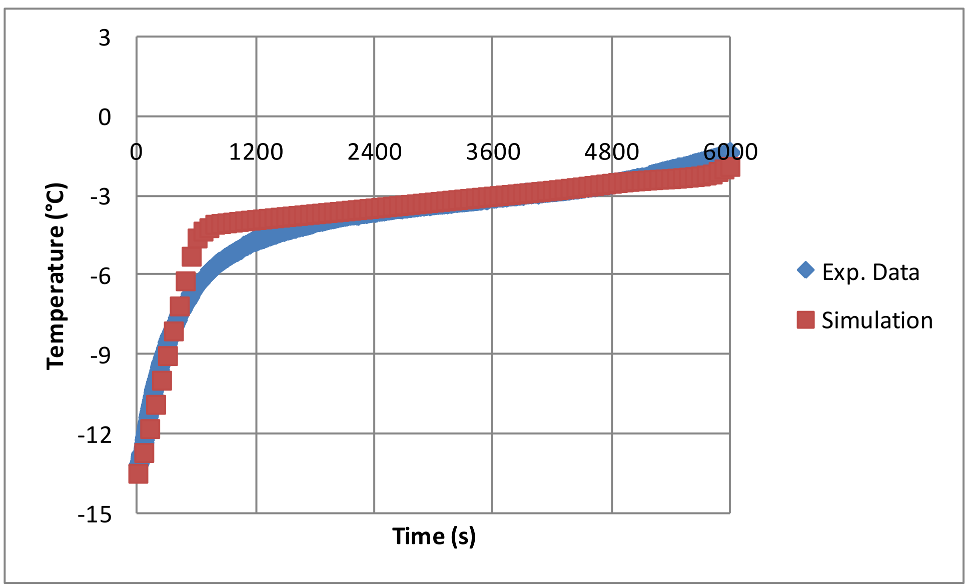

(b) - 500

Figure 8. Comparison of simulation results with the experimental data for a frozen ground lean beef block of 12.0×17.2×3.8 cm where the distance between the upper electrode and the sample surface was 12 cm.

Figure09

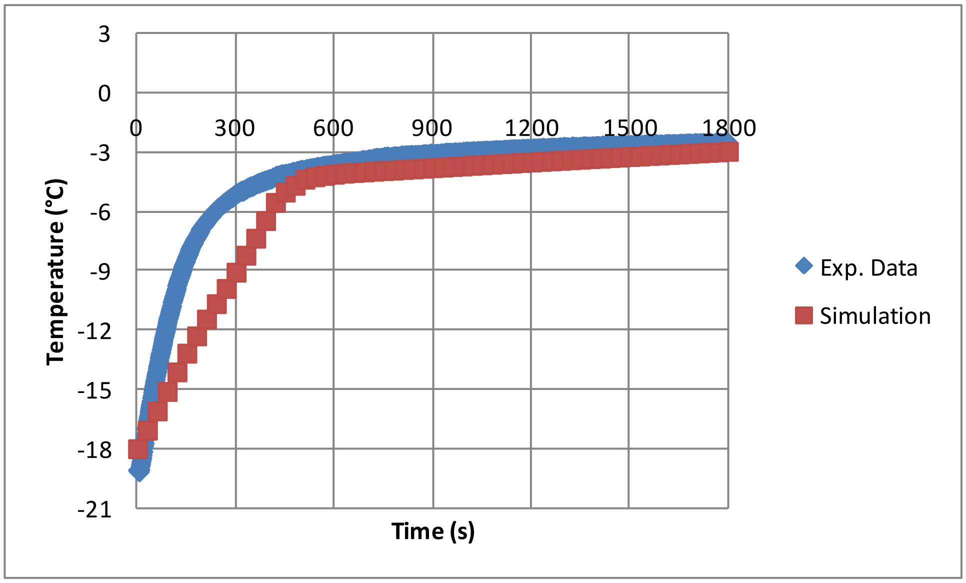

(a) - 496

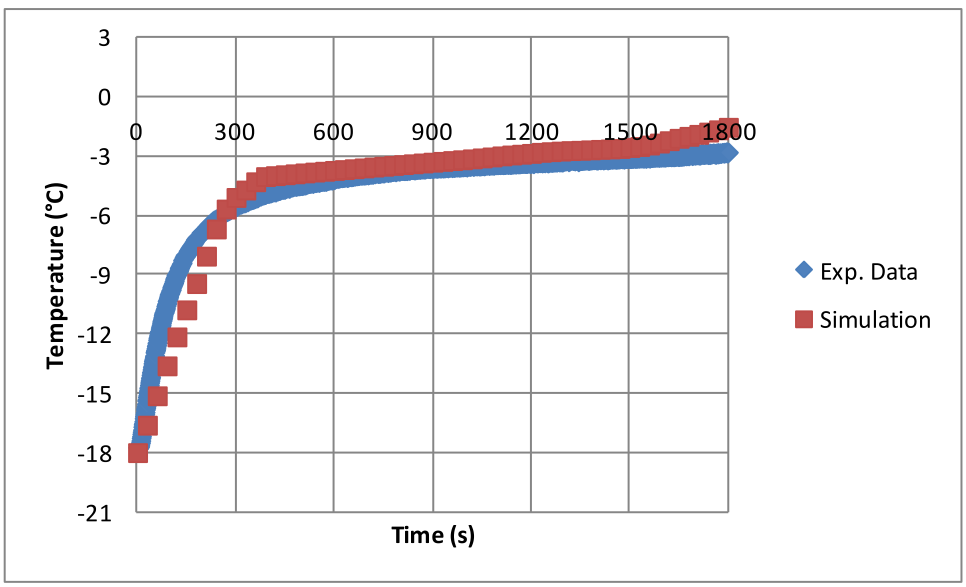

(b) - 500

Figure 9. Comparison of simulation results with the experimental data for a frozen ground lean beef block of 12.0×17.2×5.5 cm where the distance between the upper electrode and the sample surface was 13 cm.

Figure10

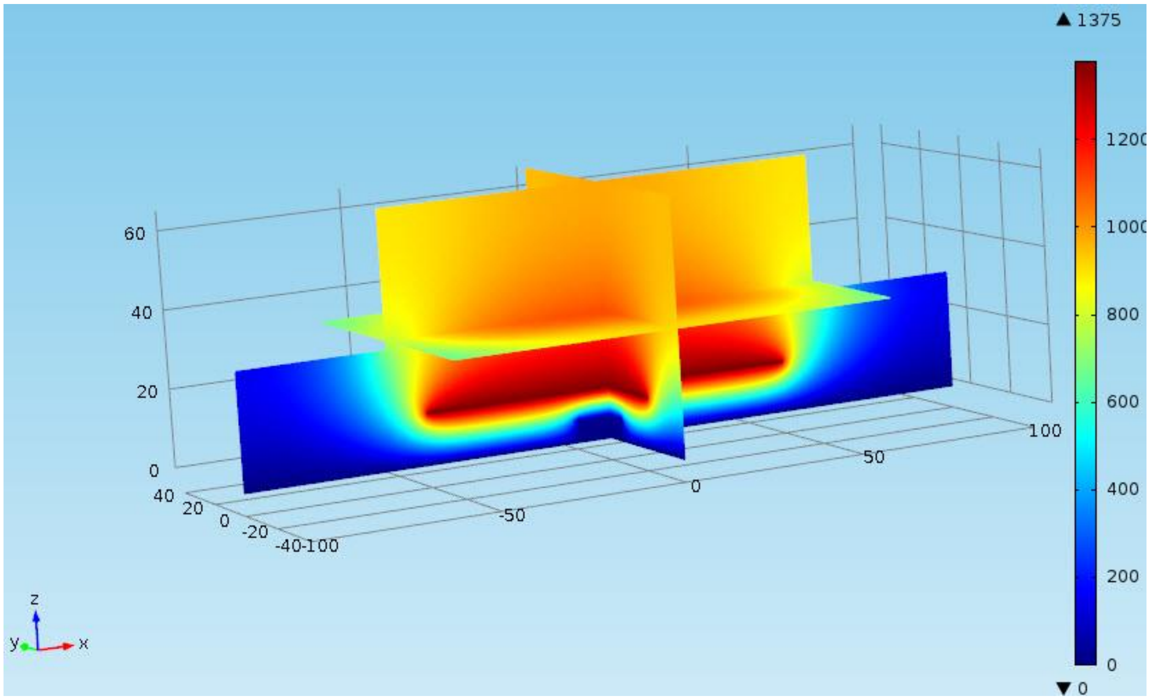

Figure 10. Electric potentaial distribution for the case of 12.0×17.2×5.5 cm sample.

Figure11

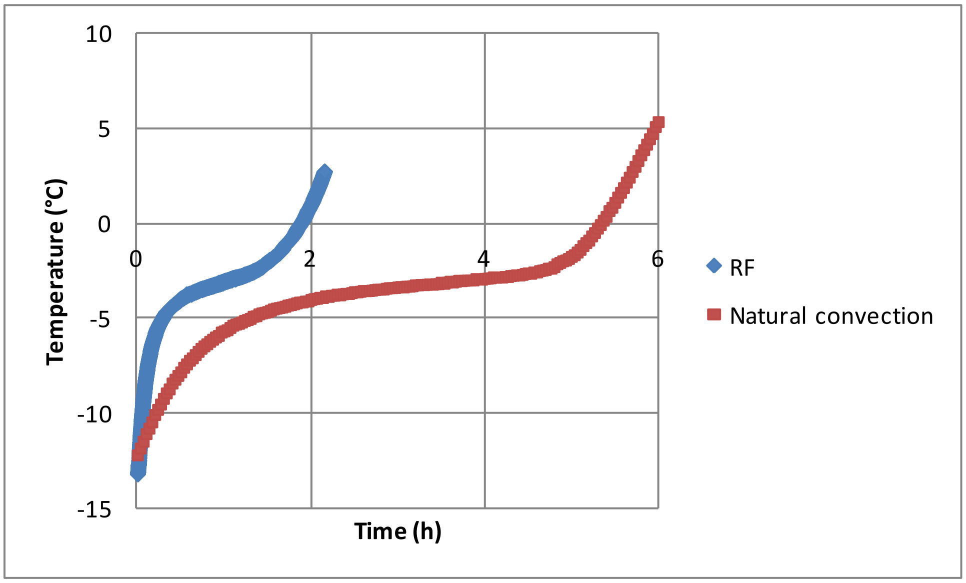

Figure 11. Comparison of radio frequency thawing with conventional natural convection thawing (experiments were conducted with the frozen block of 12.0×17.2×3.8 cm lean beef).